Femtosecond optical-pulse-induced absorption and refractive-index changes in GaAs in the midinfrared

F. Ganikhanov, K. C. Burr, D. J. Hilton, and C. L. Tang
Cornell University, Ithaca, New York 14853
(Received 26 March 1999)

We report on measurements of the ultrafast changes in the absorption and refractive index of pure GaAs in the near-infrared and midinfrared ranges of the optical spectrum. The multicolor experiments have been performed by using an ultrafast optical parametric oscillator that allowed photoexcitation of the electron-hole plasma, and probing the associated changes in both parts of the dielectric function in a wide spectral range ($\sim$1–4 μm) with femtosecond time resolution. We found that while the change in absorption is primarily due to resonant inter-valence-band optical transitions and, therefore, provides information on the dynamics of nonequilibrium holes, the corresponding refractive index change is dominated by the nonresonant Drude contribution of free carriers. Unlike the dynamics of the absorption coefficient, the time evolution of the refractive index change is found to be strongly affected by the processes of diffusion of free carriers into the bulk of the material and surface recombination. The latter effect may proceed on a picosecond time scale depending on the surface quality of the samples. We deduced from our measurements that the characteristic surface recombination velocity constant may be as high as 7.5×10^5 cm/s. [S0163-1829(99)15835-1]

I. INTRODUCTION

A detailed understanding of the relaxation mechanisms of photoexcited carriers in semiconductors is essential for various problems ranging from the development of high-speed electronic devices to fundamental questions in many-body and plasma physics. The tremendous progress of femtosecond lasers in different wavelength regions has made possible the observation of the initial stages of carrier relaxation. In particular, several studies have reported separate measurements of either electron[1] or hole dynamics[2–6] on the ultrafast time scale using multicolor, tunable femtosecond laser sources. In our work,[5,6] we have studied the evolution on the femtosecond time scale of the nonequilibrium heavy-hole, light-hole, and split-off hole (HH, LH, and SO, respectively) distributions in GaAs probed selectively in **k** space near the zone center following fs pulse-induced valence-to-conduction band (V-C) transitions. The time-resolved probe of the corresponding induced absorption in the valence band has been implemented using femtosecond pulses from a broadly tunable optical parametric oscillator (OPO) in the midinfrared which has made it possible to induce direct optical transitions between the states in the HH or LH band, and those in the SO band within a broad range of **k**-vector values.

In this paper we present our results on the measurements of the photoinduced changes in the absorption and refractive index of GaAs measured in a wide spectral range in the midinfrared. Previous studies on hole dynamics[3] based on mid-IR absorption did not examine explicitly the influence of the associated changes in the reflectivity on the time-resolved transmission signal. Our study shows that the changes in the reflectivity strongly affect the time-dependent transmission signal in the midinfrared, and should be carefully taken into account when analyzing the carrier dynamics in an uncoated semiconductor sample. We demonstrate that while the induced absorption is dominated by the band filling effect in the valence band, thus reflecting the associated nonequilibrium hole dynamics probed via resonant transitions in the band, the refractive index change is primarily due to the nonresonant Drude contribution of free carriers. The time evolution of the refractive index change, unlike that for the absorption, is found to be also influenced by carrier diffusion and surface recombination effects. Depending on the sample structure and its surface quality, these effects may proceed on a time scale as short as several picoseconds.

II. EXPERIMENT

The measurements were performed on a variety of GaAs samples using the well-known femtosecond pump-probe technique in either transmission or reflection mode. We used a thick ($d=400\,\mu$m) bulk GaAs sample ($n_e<10^{14}\,\mathrm{cm}^{-3}$) and different sample structures with GaAs epilayers in order to estimate surface recombination and diffusion effects. A high repetition rate, widely tunable femtosecond OPO using a periodically poled lithium niobate crystal[7] was used as the source of the probe radiation. The OPO was synchronously pumped by an 85-MHz repetition rate, high average power, mode-locked Ti:S laser delivering 90-fs pulses at a tunable central wavelength around 800 nm. A part of the Ti:S laser output was used as the sample pump beam, while the variable-delayed probe pulse was either the idler ($\sim$2–4 μm) or the signal ($\sim$1.0–1.3 μm) branch of the OPO output. The time resolution of the system was estimated by making cross-correlation measurements in BBO or $KNbO_3$ nonlinear crystals. Depending on the wavelength of the probe beam, typical values of the cross-correlation width (full width at half maximum) were in the range of 150–220 fs. The time-dependent $\Delta T/T$ and $\Delta R/R$ signals (or differential transmission and reflection signals) correspond, respectively, to the measured changes in the intensities of the transmitted and reflected probe beams. Using standard differential and lock-in detection techniques, the sensitivity of the system

allowed us to detect the changes in $\Delta T/T$ or $\Delta R/R$ on the level of $\sim 10^{-5}$.

III. RESULTS AND DISCUSSIONS

Taking into account the fact that without photoexcitation there is no absorption for pure bulk GaAs in the probe wavelength range and that, under moderate photoexcitation, the refractive index changes are small $[\Delta n(t) \ll n]$, the time-dependent $\Delta R/R$ for a thick sample can be represented by a simple formula

$$\frac{\Delta R(\hbar\omega_{\rm pr},t)}{R} \cong \frac{4\times\Delta n(\hbar\omega_{\rm pr},t)}{n^2(\hbar\omega_{\rm pr})-1}. \tag{1}$$

For an antireflection (AR)-coated sample ($R \approx 0$) and small changes in the absorption $[\Delta\alpha(t)]$, it can be shown that for our combination of the pump and probe photons,

$$-\left(\frac{\Delta T(\hbar\omega_{\rm pr},t)}{T}\right)\Bigg|_{R=0} \cong \Delta\alpha(\hbar\omega_{pr},t)\times d_{\rm abs}, \tag{2}$$

where $d_{\rm abs}$ is the absorption length of the pump beam. Thus measurements of $(\Delta T/T)|_{R=0}$ (i.e., for an AR-coated sample) and $\Delta R/R$ for an uncoated sample give experimentally both parts of the complex dielectric function of GaAs in the midinfrared. It is important to note that, while the differential absorption measurement gives information on processes mainly in the bulk of a sample, the $\Delta R/R$ signal is sensitive to different effects at the surface of a sample.

A. Time-dependent midinfrared absorption due to the intervalence band transitions

Neglecting free-carrier (intraband) absorption mechanisms, for the midinfrared probe photons, the differential absorption ($\Delta\alpha$) through the sample following pump-pulse-excited HH- and LH-to-*C* transitions is given by

$$\Delta\alpha_{\rm res}(\hbar\omega_{\rm pr},t) = \alpha_{\rm hh\text{-}so}(\hbar\omega_{\rm pr})\times f_{\rm hh}[E_{\rm hh}(k),t] + \alpha_{\rm lh\text{-}so}(\hbar\omega_{\rm pr}) \times f_{\rm lh}[E_{\rm lh}(k),t], \tag{3}$$

where $\alpha_{\rm hh\text{-}so}(\hbar\omega_{\rm pr})$ and $\alpha_{\rm lh\text{-}so}(\hbar\omega_{\rm pr})$ are constants proportional to the respective transition probability and joint density of states at the probe photon energy $\hbar\omega_{\rm pr} = E_{\rm hh,lh}\text{-}E_{\rm so}$. The functions $f_{\rm hh}$ and $f_{\rm lh}$ are, respectively, the distribution functions of the HH and LH bands excited by the pump beam, assuming initially empty hole bands evaluated at $E_{\rm hh}(k)$, $E_{\rm lh}(k)$, and $E_{\rm so}(k)$, the energy states in the HH, LH, and SO bands.

The absorption coefficient change in the midinfrared has been measured for a 400-μm-thick bulk GaAs sample that was antireflection coated in the 3–4-μm range. The experimental differential transmission $(\Delta T/T)|_{R=0}$ signals for this case are shown in Figs. 1(a) and 1(c) at different probe wavelengths when the pump pulse wavelength was set at $\sim$800 nm. Taking into account the valence-band structure of GaAs, with the nonparabolicity effects accounted for according to the work of Scholz,[8] the initial energies of the heavy and light holes are $\sim$15 and $\sim$55 meV, respectively. In **k**-space, these excitation energies correspond to nonequilibrium HH and LH distributions centered at $k \sim 4.5\times10^6\,{\rm cm}^{-1}$ for the HH band and $\sim 3.3\times10^6\,{\rm cm}^{-1}$ for the LH band. The corresponding wavelengths of HH-SO and LH-SO transitions involving these nonequilibrium hole distributions are centered at $\lambda_{\rm probe} \sim 3.1$ and ~ 3.8 μm, respectively. We have shown in our earlier work[5] that for the range of probe wavelengths shorter than $\sim$3.5 μm, the main contribution to $(\Delta T/T)|_{R=0}$ comes from the temporal evolution of the heavy-hole distribution. For $\lambda_{\rm probe} > 3.6$ μm, the signal is proportional to the light hole distribution function.

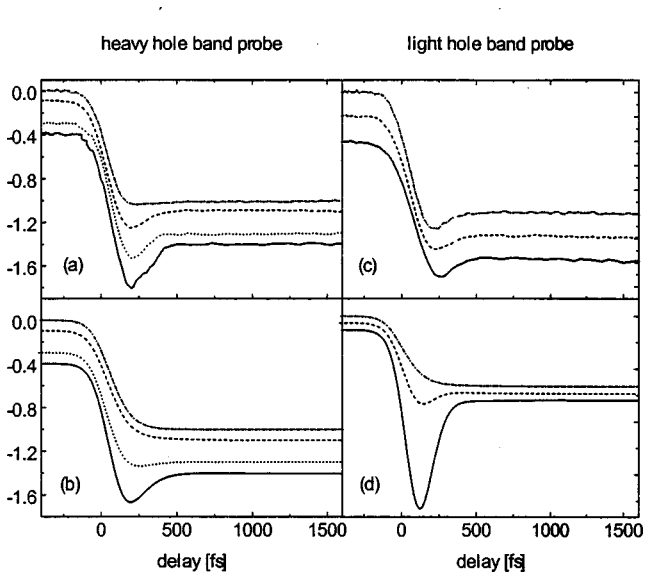

FIG. 1. The normalized measured [(a), (c)] and calculated [(b), (d)] differential transmission curves $(\Delta T/T)|_{R=0}$ for the AR-coated bulk GaAs sample for several different probe wavelengths. (a) and (b) reflect the dynamics of the heavy holes, while (c) and (d) represent the light-hole dynamics. All curves are presented on a normalized scale and offset for clarity. Heavy-hole probe wavelengths (from top to bottom): 2750 nm (—·—·—·—), 3500 nm (— — —), 3020 nm (· · · ·), and 3150 nm (——). Light-hole probe wavelengths (from top to bottom): 3600 nm (—·—·—·—), 3800 nm (· · · ·), and 4000 nm (——).

We have modeled the time-dependent absorption given by Eq. (3) on a femtosecond time scale by numerically solving the Boltzmann equation[9] for nonequilibrium hole distribution functions $f_{\rm hh}$ and $f_{\rm lh}$ under our experimental conditions. The model has been shown to give good agreement with the experimental data on hole dynamics reported in Ref. 4, where a quantitative description of the relevant scattering processes is given. In our simulation, we used an isotropic, parabolic approximation for the band structure of GaAs, with the effective mass parameters taken from Ref. 10, which lead to significant simplifications in solving the Boltzmann equations for the nonequilibrium hole distribution functions. The calculated time evolutions of the distribution functions were finally convolved with the experimental cross-correlation and the spectrum of the pulse to give the simulated $(\Delta T/T)|_{R=0}$ for comparison with our experimental results. The results of these calculations are shown in Figs. 1(b) and 1(d). In the case of probing of the heavy-hole distribution [Figs. 1(a) and 1(b)], the calculated and experimental results are in good general agreement. Both the experimental $(\Delta T/T)|_{R=0}$ signal taken at different probe wavelengths in the region of $\sim$3.0–3.4 μm (HH probe) and the calculated

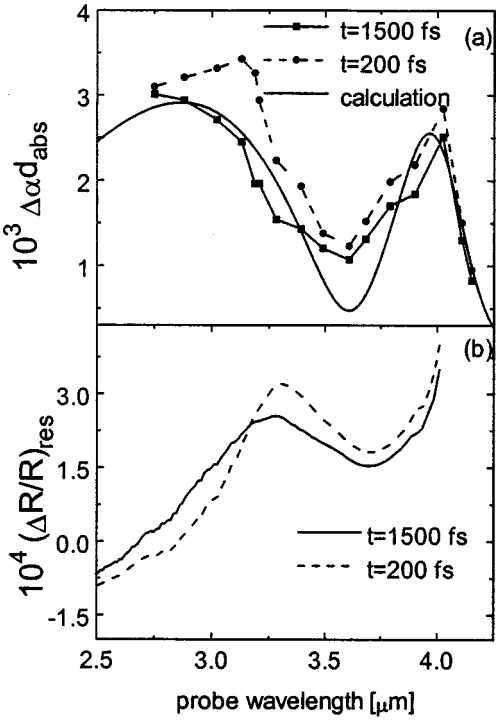

FIG. 2. (a) The experimental resonant differential absorption spectra $[-(\Delta T/T)|_{R=0} \cong \Delta\alpha \times d_{abs}]$ of the AR coated bulk GaAs sample presented for two different delay times. The photoexcited carrier density was estimated to be $\sim 2\times 10^{17}\,\mathrm{cm}^{-3}$. The solid line represents the result of calculation using Eq. (3). (b) The calculated differential reflection signal due to the corresponding resonant refractive index change based on the experimental data for $\Delta\alpha$ obtained from the data shown in the upper part of the figure and the Kramers-Kronig relations [Eq. (4)].

results show a dip at early time delays that is associated with the hole burning effect. There are, however, also some differences between the experimental and simulated results. First, the experimental result show that the hole burning structure is noticeably broader compared to the calculated signal. Second, the peak of the dip in the experimental results at 3150 nm is slightly blueshifted compared to the corresponding calculated result at 3280 nm (not shown). This slight discrepancy can be attributed to the parabolic band approximation used in the calculations. The smaller amplitude of the dip and broader hole burning structure for the experimental curves suggest higher scattering rates for the heavy-hole band. The dip in all calculated wavelengths corresponding to probing of the light-hole band (~3600–4000-nm region) appears deeper than the corresponding experimental result. A possible reason for this discrepancy is that a parabolic approximation to the light-hole band results in a lower estimated quasiequilibrium light-hole population density, which in turn, would lead to less absorption after the initial period showing the dips. We conclude, therefore, that a more rigorous model for the holes, accounting for all the above mentioned effects and including all possible scattering processes[11] using nonparabolic bands, for the light-hole band in particular, has to be applied in order to explain all the features observed in the experiment.

The magnitude of $(\Delta T/T)|_{R=0}$ versus wavelength is presented in Fig. 2(a) for delay times of 200 and 1500 fs. These time delays correspond, respectively, to the maximum negative $(\Delta T/T)|_{R=0}$ value and to the delay time when the quasiequilibrium distribution is reached. The calculated result based on Eq. (3) for slightly higher than room temperature ($T=330\,\mathrm{K}$),[12] and a photoexcited carrier density of $\sim 2\times 10^{17}\,\mathrm{cm}^{-3}$ is shown as the solid line in Fig. 2. We also assumed a quasiequilibrium distribution for holes, and have taken into account our probe pulse bandwidth. The calculation provided only a relative value of the absorption; the resulting absorption curve was scaled to match the experimental data. The result is in general agreement with the experimental data. The discrepancies are attributed to experimental error and to the fact that certain band-structure properties (e.g., warping and nonparabolic effects, etc.) were not accounted for in this calculation. Apart from these points, there is possibly a small contribution due to free carrier (intraband) absorption, which is discussed below. We also note that the shape of the theoretical curve is found to be sensitive to the sample temperature and probe pulse bandwidth variations, which might not have been accounted for properly. The absolute value of the experimentally measured absorption at our typical excitation density of $\sim 2\times 10^{17}\,\mathrm{cm}^{-3}$ is about 10–30 cm^{-1} in the wavelength range of ~3–4 μm, in good agreement with previous linear absorption experiments on *p*-doped GaAs.[13] A characteristic minimum in the absorption dependency versus wavelength is observed at ~3.6 μm. This wavelength corresponds to probing at the zone center where $\alpha_{\mathrm{hh\text{-}so}}(\hbar\omega_{\mathrm{pr}})$ and $\alpha_{\mathrm{lh\text{-}so}}(\hbar\omega_{\mathrm{pr}})$ vanish because of selection rules. For wavelengths longer than ~4 μm (~ 0.3 eV), the absorption drops sharply because of the absence of resonant transitions between the states in the HH/LH bands and those in the SO band. It is worth noting that the drop in the absorption for wavelengths longer than 4 μm in our pure GaAs samples is significantly deeper than that reported in Ref. 13 on *p*-doped GaAs.

We believe that the free-carrier (intraband) absorption mechanism is too weak to affect our experimental data significantly. Based on data from the review paper by Blakemore,[10] we estimate that, for the carrier density excited in our experiment, the free-carrier absorption coefficient at wavelengths between 3 and 4 μm is on the order of 1–2 cm^{-1}. This absorption level is far less than the induced absorption observed in our experiment. Even at λ_{probe} ~4.3 μm, where the measured absorption has fallen significantly from its peak level, the $(\Delta T/T)|_{R=0}$ measurements indicate that the absorption coefficient is on the level of 7–10 cm^{-1}, or approximately an order of magnitude greater than the estimated free-carrier absorption.

Thus the observation of spectral hole burning, a characteristic minimum in the probe wavelength dependence of the induced absorption, and a sharp drop in the absorption beyond 4 μm confirm that, in pure GaAs, the absorption in the midinfrared up to 4 μm is due to the two different intervalence band transitions, namely, HH-to-SO and LH-to-SO band transitions. Because HH transitions dominate in one wavelength region (<3.5 μm) and LH transitions dominate in another (>3.6 μm), and neither transition is affected directly by the conduction band population distribution, the multiwavelength pump-probe technique described here can provide independent information about the ultrafast evolution of the HH and LH population distributions.

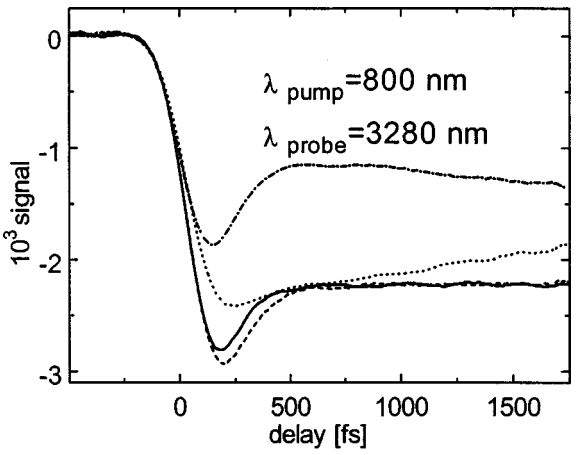

FIG. 3. Measured $\Delta R/R$ (dotted line) and $\Delta T/T$ (dash-dotted line) curves for the uncoated GaAs sample at a probe wavelength of ~3.3 μm. The dashed curve corresponds to $-\Delta\alpha\times d_{\text{abs}}$ where $\Delta\alpha$ is determined, making use of the results of Ref. 14, from the measured $\Delta T/T$ and $\Delta R/R$ for an uncoated sample. The corresponding measured $(\Delta T/T)|_{R=0}$ signal for the AR-coated GaAs sample (solid line) is plotted for comparison [See Eq. (2)].

B. Mid-IR resonant refractive index change

With the knowledge of the dispersion of the absorption coefficient due to the resonant transitions in the valence band, the corresponding changes of the resonant refractive index (Δn_{res}) can be estimated using the Kramers-Kronig relation

$$\Delta n_{\text{res}}(\omega)=\frac{c}{4\pi}P\int_0^{\infty}\frac{\Delta\alpha(\omega')d\omega'}{\omega'^2-\omega^2}, \tag{4}$$

where c is the speed of light, and P denotes the principal value of the integral. The calculated $(\Delta R/R)_{\text{res}}$ based on such calculated Δn_{res} using Eqs. (1) and (4) is shown in Fig. 2(b). The corresponding magnitude of the $(\Delta R/R)_{\text{res}}$ signal is approximately an order of magnitude smaller than that of the measured $(\Delta T/T)|_{R=0}$ signal. Therefore, the contribution to the differential reflectivity signal *due to the induced resonant refractive index change* is not expected to noticeably affect the corresponding differential transmission signal for the uncoated sample (which we denote as $\Delta T/T$ below).

C. Refractive index change due to the Drude contribution of free carriers

The experimental data for the uncoated sample presented as an example in Fig. 3 show, however, that the differential absorption signal is strongly influenced by the corresponding changes in the reflectivity. The latter is of the same order of magnitude as, and has a strong effect on, the temporal profile of $\Delta T/T$ (dash-dotted curve in Fig. 3), thus making it noticeably different from the corresponding $(\Delta T/T)|_{R=0}$ (solid curve in Fig. 3) for the AR-coated sample. Properly accounting for the influence of reflectivity on the differential absorption signal,[14] we can deduce the transmission signal due to bulk absorption (i.e., $-\Delta\alpha\times d_{\text{abs}}$) shown as the dashed line in Fig. 3. Good agreement between this curve and the experimentally measured $(\Delta T/T)|_{R=0}$ signal for the coated sample (solid line) can be seen in Fig. 3.

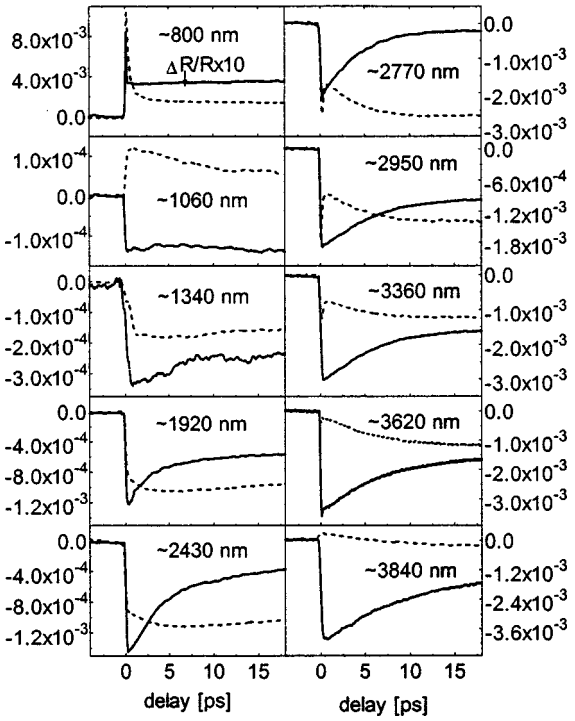

FIG. 4. Measured $\Delta R/R$ (solid line) and $\Delta T/T$ (dashed line) signals for the uncoated 5-μm-thick GaAs epilayer sample at different probe wavelengths following photoexcitation by the pump pulse ($\lambda_{\text{pump}}\sim 800$ nm). The near-surface carrier density was estimated to be $\sim 2\times 10^{17}\,\text{cm}^{-3}$.

Apart from the contribution to the differential reflectivity signal due to Δn_{res} there is the contribution originating from the refractive index change due to the Drude contribution of free carriers excited in the sample. Within this model,[15,16] the change in the real part of the dielectric function due to the free carriers in the high-frequency limit is given by

$$\Delta\varepsilon\cong-\frac{4\pi e^2}{\omega_{\text{pr}}^2}\left[\sum_c\frac{N_c(t)}{m_c}+\sum_v\frac{N_v(t)}{m_v}\right], \tag{5}$$

where the sums are over all conduction (c) and valence (v) bands, $N_{c,v}$ are the carrier densities in each band, and $m_{c,v}$ are the respective effective masses.

We have made differential absorption and reflectivity measurements at several different probe wavelengths. The results are shown in Fig. 4 on a picosecond time scale. These measurements and the related discussion given below provide a global view of the ultrafast absorption and refractive index properties of pure GaAs in the midinfrared.

The measured ultrafast responses in the upper left corner of the figure correspond to pump and probe wavelengths centered at ~800 nm. The $\Delta T/T$ curve for this combination of wavelengths is for a sample structure consisting of 0.27 μm of GaAs epilayer between two $Al_{0.75}Ga_{0.25}As$ layers. A 5-μm-thick GaAs epilayer sample grown on a GaAs substrate has been chosen for the corresponding $\Delta R/R$ measurement in order to avoid etalon effects. Apart from the magnitude of the signals, they, in general, exhibit similar temporal

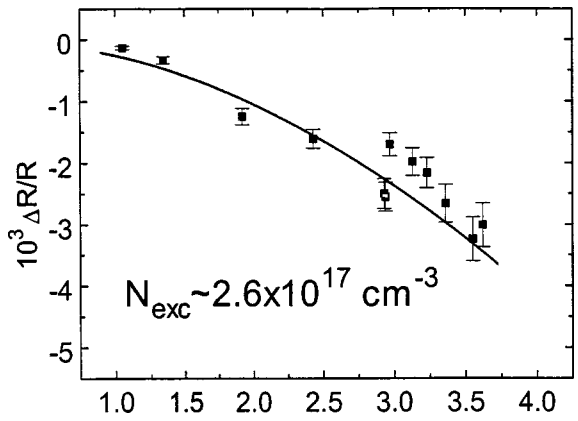

FIG. 5. The magnitude of the $\Delta R/R$ signal vs wavelength for an uncoated 5-μm-thick GaAs epilayer. The photoexcited carrier density was $\sim 2\times 10^{17}\,\mathrm{cm}^{-3}$. The solid line represents the calculated curve using the Drude model [Eq. (5)].

shape suggesting that, for this probe wavelength, both the absorption and refractive index changes are of the same origin, namely, a resonant transition between optically coupled states in the valence and conduction bands. For this case, the free-carrier contribution estimated with the help of Eq. (5) is more than an order of magnitude smaller than the observed $\Delta R/R$ signal, and, therefore, has a barely noticeable effect on the signal when comparing the details of the time evolution of the $\Delta T/T$ and $\Delta R/R$ signals at short time delays. Also, for the interband transition, many-body effects have been reported to contribute to the observed differences in time behavior of the absorption and refractive indexes changes.[17]

The remaining traces in Fig. 4 show the measured results at longer probe wavelengths, where there is no appreciable contribution from the valence-to-conduction (V-C) band transitions. For example, in the case of $\lambda_{\mathrm{probe}}\sim 1060$ nm (1.17 eV), the corresponding $\Delta R/R$ signal becomes negative and its magnitude is of the same order as that expected for the free carrier contribution. We believe that the variation in the corresponding $\Delta T/T$ signal (dashed curve) is mainly due to the influence of the reflectivity changes and is, therefore, an inverted replica of the reflectivity signal. However, resonant intervalence band transitions and, to a much lesser extent, contributions due to near-resonant V-C transitions are probably also important, since certain differences are observed in the time dependence of the two signals ($\Delta R/R$ and $\Delta T/T$) at longer time delays. At wavelengths somewhat longer than $\lambda_{\mathrm{probe}}\sim 1.34\,\mu$m, the onset of the induced intervalence band absorption is clearly seen. We note that the induced intervalence band absorption for the wavelength range of 1.33–1.58 μm has been observed earlier in picosecond time-domain experiments,[18] although absorption stronger (by approximately a factor of 3) than that seen in our study was reported. The $(-\Delta R/R)$ signal increases continuously with the probe wavelength, and the change in the $\Delta T/T$ signal is dominated by the effect due to the change in $\Delta R/R$ as can be seen for probe wavelengths longer than $\sim$3.6 μm. As for the magnitude (peak value) of the $\Delta R/R$ signal (see Fig. 5), good agreement is found between the experimental and theoretical curves based on Eq. (5), where the effective mass parameters for the GaAs bands have been taken from the review paper by Blakemore[10] and the carrier densities for the corresponding bands after photoexcitation have been estimated using Boltzmann rate equations for the distribution functions of the carriers.[19] We attribute the small differences between the experimental data and calculated curve shown in Fig. 5 to the corresponding contribution to $\Delta R/R$ due to the resonant refractive index change [see Fig. 2(b)]. Thus we conclude that, in the midinfrared, the differential reflectivity signal is almost entirely due to the nonresonant refractive index changes associated with the Drude contribution of free carriers.

D. Time evolution of the differential reflectivity signal

The nonresonant contribution to $\Delta R/R$ is related to the change in the index of refraction at the entrance facet, $\Delta n(z=0,t)$, due to the Drude contribution of free carriers. Its time dependence is determined by that of the free-carrier density, $N(z=0,t)$, at the interface which is, in turn, determined by the bulk and surface diffusion processes. Assuming charge neutrality and neglecting the slower bulk radiative recombination effect, these diffusion effects are well described by the equation

$$D\nabla^2 N(z,t)-\frac{\partial}{\partial t}N(z,t)=-g(z,t) \tag{6}$$

subject to the boundary condition

$$D\frac{\partial}{\partial z}N(z,t)\big|_{z=0}=SN(0,t), \tag{7}$$

where D is the ambipolar diffusion constant, S is the surface velocity, and $g(z,t)$ is the generating function for the pump-photon excited carriers. It can be shown[20] that Eqs. (6) and (7) lead to the following integral equation for the carrier density at the surface, $N(0,t)$, assuming no transverse variation:

$$N(0,t)=\int_{-\infty}^{t}\int_{0}^{\infty} g(z_0,t_0)G(0,t|z_0,t_0)\,dt_0\,dz_0 - S\int_{-\infty}^{t} N(0,t_0)G(0,t|0,t_0)\,dt_0, \tag{8}$$

where

$$G(z,t|z_0,t_0)=\frac{1}{2\sqrt{\pi D(t-t_0)}}\left\{\exp\left[-\frac{(z-z_0)^2}{4D(t-t_0)}\right]+\exp\left[-\frac{(z+z_0)^2}{4D(t-t_0)}\right]\right\} \tag{9}$$

is the Green's function satisfying the equation

$$D\frac{\partial^2}{\partial z^2}G(z,t|z_0,t_0)-\frac{\partial}{\partial t}G(z,t|z_0,t_0)=-\delta(z-z_0)\,\delta(t-t_0), \tag{10}$$

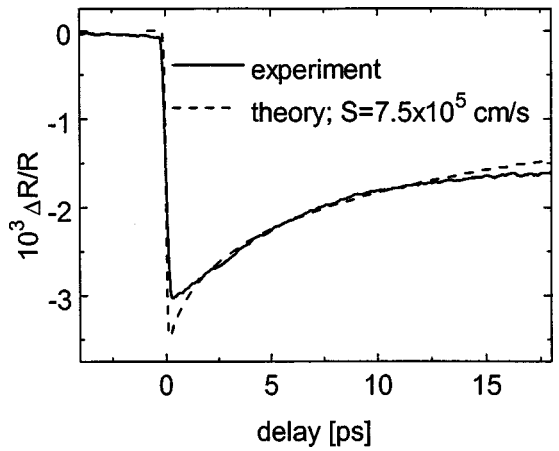

FIG. 6. The measured $\Delta R/R$ signal taken at a probe wavelength of ~ 3.35 μm (solid line). The dashed curve represents the calculated result based on Eqs. (1), (5), and (6)–(11). The best fit corresponds to the surface recombination velocity constant of $\sim 7.5 \times 10^5$ cm/s.

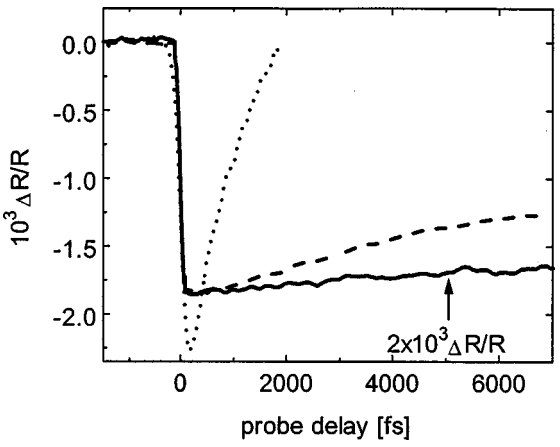

FIG. 7. Differential reflectivity data demonstrating the influence of the surface recombination effect for samples of different surface quality: solid line, 0.27-μm-thick epilayer sandwiched between $Al_{0.75}Ga_{0.25}As$ layers; dashed line, 5-μm thick GaAs epilayer grown on a GaAs substrate; dotted line, GaAs substrate material mechanically polished using aluminum oxide powder (0.3-μm particle diameter).

with the boundary condition

$$\frac{\partial}{\partial z_0} G(z,t|z_0,t_0)\big|_{z_0=0} = 0. \tag{11}$$

Equation (8) can be solved by numerical iteration. We assume that the time dependence of $g(z_0,t_0)$ follows the temporal profile of the pump pulse, and its spatial dependence is of the form $\exp(-\alpha z_0)$, where α is the intensity attenuation constant of the pump photon in the medium. Assuming a temperature-independent ambipolar diffusion constant of $D = 17\ \mathrm{cm}^2/\mathrm{s}$ (Ref. 21) and $\alpha \sim 1.36 \times 10^4\ \mathrm{cm}^{-1}$ (for $\lambda \sim 800$ nm),[22] the value of the surface-velocity parameter S that leads to the best fit between the calculated results and the experimental data beyond ~ 1 ps is approximately 7.5×10^5 cm/s, which is consistent with results reported in the literature.[23] An example of the calculated $\Delta R/R$ based on such a numerical solution is shown in Fig. 6 along with the corresponding experimental results for an uncoated 5-μm-thick GaAs epilayer. We attribute the observed discrepancy in the subpicosecond range to carrier-carrier and carrier-phonon scattering processes of hot carriers initially excited by the pump pulse. The effect of high-carrier temperature on the diffusion process in Ge has been reported previously.[24]

To confirm that the surface recombination effect plays a significant role in the decay of our differential reflectivity signal, we have carried out measurements on GaAs samples with different surface preparations and qualities. The results are shown in Fig. 7. For a bulk sample with a relatively rough mechanically polished (aluminum oxide powder with a particle size diameter of ~ 0.3 μm) surface, a faster decay constant on the order of a few picoseconds with a corresponding surface velocity parameter of 5×10^6 cm/s is seen. On the other hand, for a high-quality 0.27-μm GaAs epilayer capped by a thin $Al_{0.75}Ga_{0.25}As$ layer, a much slower decay constant is observed. These results suggest also that picosecond measurement of the time-dependence of the midinfrared surface reflectivity could be used as a technique to probe the surface quality of a semiconductor sample.

IV. CONCLUSIONS

In conclusion, we have measured the time-dependent changes in the absorption and refractive index in bulk GaAs in the midinfrared range due to photoexcited carriers using a two-wavelength pump-probe technique in the transmission and reflection modes. The changes in the midinfrared absorption are caused by band-filling effects in the valence band and are sensitive to the associated carrier dynamics. Because HH transitions dominate in one wavelength region (<3.5 μm) and LH transitions dominate in another (>3.6 μm), and neither transition is affected directly by the conduction-band population distribution, the multiwavelength pump-probe technique described here can provide independent information about the ultrafast evolution of the HH and LH population distributions. Our simultaneous transmission and reflection measurements illustrate, however, that for this technique to yield accurate absorption measurements, the changes in midinfrared reflectivity must be reduced (by using AR-coated samples) or accounted for properly. The refractive index changes in the optical spectral range of 1–4 μm are due to the Drude contribution of free carriers photoexcited in the sample, and their time evolution is governed primarily by the processes of carrier diffusion and surface recombination. The latter process proceeds on a time scale of a few picoseconds depending on the surface quality of the samples.

ACKNOWLEDGMENTS

The authors thank F. Vallée for many helpful discussions and for the computer code used to calculate the results shown in Fig. 1, and J. Prineas, H. Gibbs, and A. Schremer for the GaAs samples used in these experiments. This work was supported by the National Science Foundation and the Joint Services Electronics Program.

[1] F. X. Camescasse, A. Alexandrou, D. Hulin, L. Banyai, D. B. Tran Thoai, and H. Haug, Phys. Rev. Lett. **77**, 5429 (1996).
[2] K. Meissner, B. Fluegel, R. Binder, S. W. Koch, G. Khitrova, and N. Peygambarian, Appl. Phys. Lett. **59**, 259 (1991).
[3] M. Woerner, W. Frey, M. T. Portella, C. Ludwig, T. Elsaesser, and W. Kaiser, Phys. Rev. B **49**, 17 007 (1994); M. Woerner and T. Elsaesser, *ibid.* **51**, 17 490 (1995)); Z. Xu, P. M. Fauchet, C. W. Rella, B. A. Richman, H. A. Schwettman, and G. W. Wicks, *ibid.* **51**, 10 631 (1995).
[4] P. Langot, R. Tommasi, and F. Vallée, Phys. Rev. B **54**, 1775 (1996).
[5] F. Ganikhanov, K. C. Burr, and C. L. Tang, Appl. Phys. Lett. **73**, 64 (1998).
[6] K. C. Burr and C. L. Tang, Appl. Phys. Lett. **74**, 1734 (1999).
[7] K. C. Burr, C. L. Tang, M. A. Arbore, and M. M. Fejer, Appl. Phys. Lett. **70**, 3341 (1997); Opt. Lett. **22**, 1458 (1997)
[8] R. Scholz, J. Appl. Phys. **77**, 3219 (1995).
[9] J. Collet and T. Amand, J. Phys. Chem. Solids **47**, 153 (1986).
[10] J. S. Blakemore, J. Appl. Phys. **53**, R123 (1982).
[11] *Inter-valence-band* scattering induced by carrier-carrier interaction and carrier acoustic-phonon interaction has been neglected in our calculations.
[12] Using a thermopile we have found that the surface temperature of the samples is generally higher (by ~25–40 K) than room temperature due to heating by the pump beam. For our pump geometry, the carrier density mentioned in the text corresponded to an average pump beam power of ~100 mW.
[13] R. Braunstein and E. O. Kane, J. Phys. Chem. Solids **23**, 1423 (1962).
[14] S. Hunsche, H. Hessel, and H. Kurz, Opt. Commun. **109**, 258 (1994).
[15] P. Y. Yu and M. Cardona, *Fundamentals of Semiconductors* (Springer, Berlin, 1996).
[16] G. Abstreiter, M. Cardona, and A. Pinczuk, in *Light Scattering in Solids IV*, edited by M. Cardona and G. Güntherodt (Springer-Verlag, Berlin, 1984).
[17] T. Gong, W. L. Nighan, Jr., and P. M. Fauchet, Appl. Phys. Lett. **57**, 2713 (1990).
[18] M. Pugnet, J. Collet, and B. Saint Cricq, Europhys. Lett. **7**, 567 (1988).
[19] F. Vallée (unpublished).
[20] P. Morse and H. Feshbach, *Methods of Theoretical Physics* (McGraw-Hill, New York, 1983), p. 859
[21] A. Olsson, D. J. Erskine, Z. Y. Xu, A. Schremer, and C. L. Tang, Appl. Phys. Lett. **41**, 659 (1982).
[22] E. D. Palik, *Handbook of Optical Constants of Solids* (Academic, Orlando, 1985).
[23] D. C. Marvin, S. M. Beck, J. E. Wessel, and J. G. Rollins, IEEE J. Quantum Electron. **25**, 1064 (1989).
[24] A. Othonos, H. M. van Driel, J. F. Young, and P. Kelly, Phys. Rev. B **43**, 6682 (1991).